RESEARCH ARTICLE

Osteogenic differentiation and biocompatibility of rabbit bone marrow mesenchymal stem cells promoted by hydroxyapatite-chitosan composites

Linlin Yang, Yuting He, Jiaxin Huang, Wenxin Li, Wenjing Xie, Jiafu Huang*

Collaborative Innovation Center of Mushroom Health Industry, Engineering Technological Center of Mushroom Industry, School of Life Sciences and Biotechnology College, Minnan Normal University Zhangzhou, Fujian 363000, China

Received: January 25, 2022; **accepted:** February 17, 2021.

Hydroxyapatite (HA) is the main inorganic component of hard tissues such as human bones and teeth and has been widely used in tissue engineering scaffolds. Chitosan (CS) is an alkaline polysaccharide from a wide range of natural sources and has good adsorption properties for a wide range of metal ions. Bone marrow mesenchymal stem cells (BMSCs) are cells with a self-renewing, multidirectional differentiation potentials and may differentiate into chondrocytes, osteoblasts, adipocytes, neuronal cells, fibroblasts, *etc*. under different induction conditions. This study investigated the effects of hydroxyapatite-chitosan (HA-CS) composites on the growth, proliferation, and differentiation of BMSCs to find suitable stem cell carriers as donor materials for bone transplantation and repair. BMSCs were isolated, cultured, and purified *in vitro* by the whole bone marrow apposition method. The effects of HA, CS, and HA-CS on the proliferation of BMSCs were investigated by MTS assay. The amount of bone forming protein 2 (BMP-2) in the process of differentiation of BMSCs into osteoblasts was measured experimentally. The number of induced mineralized nodules was evaluated by Von-Kossa modified staining method. The results showed that, in terms of biocompatibility, there was no significant increase or decrease in the proliferation rate of BMSCs after HA, CS, and HA-CS incubations. The cell morphology tended to gradually fuse into sheets comparing to the blank control group. In terms of induction of osteoblasts, BMP-2 expression was upregulated, and the number of formed mineralized nodules was significantly increased with HA-CS demonstrating the most significant effect. The results confirmed that HA-CS composite showed good histocompatibility and promoted differentiation towards osteoblasts.

Keywords: hydroxyapatite; chitosan; bone marrow mesenchymal stem cells; osteogenic differentiation; biocompatibility.

***Corresponding author:** Jiafu Huang, Collaborative Innovation Center of Mushroom Health Industry, Minnan Normal University, Zhangzhou, Fujian 363000, China. Phone: +86 596 252 3230. E-mail: dongxie1982@qq.com.

Introduction

Bone defects that are caused by trauma, ageing, and disease are currently repaired by using autogenous bone, allogeneic bone, and allograft bone grafts. Autologous bone sources are insufficient and have donor area complications. Both allogeneic and xenogeneic bones may have immune rejection and the risk of spreading disease [1-4]. Therefore, there is necessary to develop artificial bone repair materials that can promote the repair or regeneration of damaged bone tissue. The ideal bone repair materials should have the following criteria: (1) biocompatibility, which does not cause immune rejection after transplantation into the body; (2)

degradability, the material degrades *in vivo* and is eventually replaced by its own bone, providing support during the degradation process, and acting as a scaffold for new bone formation; (3) appropriate surface properties and porosity, simulating the composition, structure, and properties of biological bone tissue with specific pore size and porosity to facilitate material exchange; (4) osteoconductive and its properties, inducing differentiation of mesenchymal cells from adjacent tissues into osteoblasts or facilitating crawling of adjacent bone tissue [5-8]. Hydroxyapatite (HA), the main inorganic component of natural bone tissue, has excellent biocompatibility and osteoconductivity, and can be directly chemically bonded to surrounding hard tissues to increase bone adhesion, making it one of the ideal matrix materials for artificial bone repairing [9, 10]. However, HA, as a bone repair material, still has the following problems: (1) differences in pore structure and active ingredients comparing to natural bone; (2) slow degradation after implantation; and (3) low mechanical strength. Increasing chitosan (CS) can improve the biophysical and biological characteristics of HA if the two composite materials were combined (HA-CS) [11-13]. This study evaluated the histocompatibility of HA-CS and induced differentiation of bone marrow mesenchymal stem cells (BMSCs) to osteoblasts by HA-CS to explore the potentially new materials for the artificial bone repairing.

Materials and methods

Primary isolation and culture of BMSCs

Five male healthy and specific pathogen free level New Zealand White rabbits with the average body weight of 1.0 ± 0.2 Kg were purchased from the Shanghai Experimental Animal Center of the Chinese Academy of Sciences (Qualification No.: SCXK(Shanghai)2012-0002). The disposal of the animals during the experiment was in accordance with the standard of "Guiding Opinions on the Good Treatment of Laboratory Animals" issued by the Ministry of Science and Technology of the People's Republic of China in 2006. Briefly, 3% pentobarbital sodium was applied to anesthetize rabbits, and the whole body was shaved and put into 75% ethanol for 15 min for disinfection. The femur and tibia were taken under aseptic conditions, the epiphyses of the femur and tibia were cut off to expose the bone marrow cavity. The bone marrow was flushed out with Dulbecco's modified eagle medium (DMEM) (Thermo Fisher, Waltham, MA, USA) with the addition of 100 U of penicillin, 100 U of streptomycin, and 12% fetal bovine serum (FBS), and repeatedly blown. The flushed bone marrow was made into a single cell suspension by centrifuged at 1,000 rpm for 5 min. The supernatant was discarded. The pellet was resuspended at a concentration of 1×10^9 cells/L in a 75 cm^2 culture flask and incubated in FORMA 3111 CO_2-incubator (Thermo Fisher, Waltham, MA, USA) at 37℃ [15, 16].

Culture and passaging of BMSCs

After 48 h of apposition, the medium was replaced, and the medium was changed every 3 days during the culture. When the cell fusion reached 70%-80%, the cells were digested with 0.25% trypsin and passaged in a ratio of 1:2.

Morphological observation of BMSCs

The morphological changes and growth of the cells were observed daily with an Olympus IX51 inverted phase contrast microscope (Olympus, Shinjuku, Japan) during the culture process and recorded. The purified 2^{nd} generation cells were adjusted to a cell concentration of 5×10^7 cells/L and were inoculated into 6-well plates with 1 mL per well. When the cells were evenly distributed and about 80% fused, the cells were washed 3 times with phosphate buffer saline, fixed with methanol for 10 min, stained with Giemsa staining solution (Sigma-Aldrich Chemie GmbH, Taufkirchen, Germany) for 5 min, rinsed with distilled water, and observed under the inverted microscope for photographs [17].

Growth curve of BMSCs

BMSCs in good growth and passed to the second generation were inoculated in 96-well plates at a density of 5×10^3 cells/well and incubated in a

CO_2-saturated humidity incubator at 37℃. 20 μL 3-(4,5-dimethylthiazol-2-yl)-5-(3-carboxymethoxyphenyl)-2-(4-sulfophenyl)-2H-tetrazolium (MTS) (Promega, Madison, WI, USA) was added daily, and the OD value was measured at 492 nm on Infinite M200 Pro multimode microplate reader (TECAN, Männedorf, Swiss) after mixing for 4 h. The results were recorded, and the cell growth curve was plotted with time as the horizontal axis and OD value as the vertical axis [18].

Cell cycle assay of BMSCs

The 3rd generation cells were taken, and the cell concentration was adjusted to 1.0×10^6 cells/L. The cell cycle was detected by Flowsight flow cytometry (Millipore, Burlington, MA, USA) according to the instructions of the cycle test kit (Beyotime, Shanghai, China) [19].

***In vitro* directed induction of differentiation of BMSCs**

The 3rd generation BMSCs were selected and inoculated in 6-well cell culture plates at a concentration of 1×10^8 cells/L. When the cell adheres to the wall and grows to 80% cell density, the lipogenic cell inducers (1 mmol/L dexamethasone, 10 mg/L insulin, 50 mmol/L 3-isobutyl-1-methylxanthine (IBMX), and 0.2 mmol/L indomethacin) and osteoblast inducers (1 mmol/L dexamethasone, 1 mol/L sodium β-glycerophosphate, 50 mmol/L ascorbic acid) were added to the complete culture medium of each induction well, respectively. The medium of each induction well was changed twice a week, and the cell culture well without induction medium was used as the blank control group. After 18 days of lipogenic cell inducer induction, the induced differentiated adipocytes were fixed by 40 g/L paraformaldehyde and stained with Oil Red O (0.3% Oil Red, 60% isopropyl alcohol). After 21 days of osteoblast inducer induction, the induced differentiated osteoblasts were fixed by 40 g/L paraformaldehyde and stained with Von-Kossa modified staining (5% silver nitrate, 5% sodium thiosulfate) [20].

Effect of HA-CS on the proliferation of BMSCs

The 3rd generation BMSCs with logarithmic growth phase cells were selected. The cell concentration was adjusted to 2.0×10^4 cells/mL and was inoculated in 96-well plates with 100 μL per well and incubated at 37℃, saturated humidity, 5% CO_2 sterile incubator for 24 h and then replace the culture solution. In the experimental group, 200 μL of HA and CS extracted from *Agaricus bisporus*, and HA-CS composite synthesized by the inverse emulsion cross-linking method and prepared by the ultrasonic-assisted chemical precipitation method were added, respectively. The blank control group was only added 200 μL of culture medium (10% FBS and DMEM). Six parallel replicate wells were set up for each group, and after incubation for 24, 48, 72, and 96 h, 20 μL of MTS solution was added and the incubation was continued for 4 h. The absorbance (A value) was measured at 492 nm on multimode microplate reader, and the cell proliferation rate was calculated as follows:

$$\text{Cell proliferation rate (\%)} = \frac{A_{\text{experiment}} - A_{\text{experiment blank control}}}{A_{\text{control}} - A_{\text{blank group}}} \times 100\%$$

All the experiments were repeated three times.

Effect of HA-CS on the differentiation of BMSCs to osteoblasts

The 3rd generation BMSCs were selected and inoculated into 6-well cell culture plates at a concentration of 1×10^8 cell/L. When the cells grew against the wall and the cell density reached 80%, the culture medium was replaced. The leachates of HA, CS, and HA-CS were prepared by adjusting the pH of HA, CS, and HA-CS to 6.8 and sterilizing at 121.3℃ for 15 min. The solubility of HA, CS, and HA-CS was achieved at 0.2 g/mL by using cell culture solution (10% FBS and DMEM) as solvent. The mixture solution was placed in CO_2-incubator at 37℃ and 5% CO_2 for 24 h before filtering with 0.22 μm filter. The filtrate was stored at 4℃ for following experiments [14]. 1 mL of each HA and CS extracts and HA/CS composite was added into the experimental group. The blank control group was only added 1 mL of culture medium (10% FBS and DMEM)

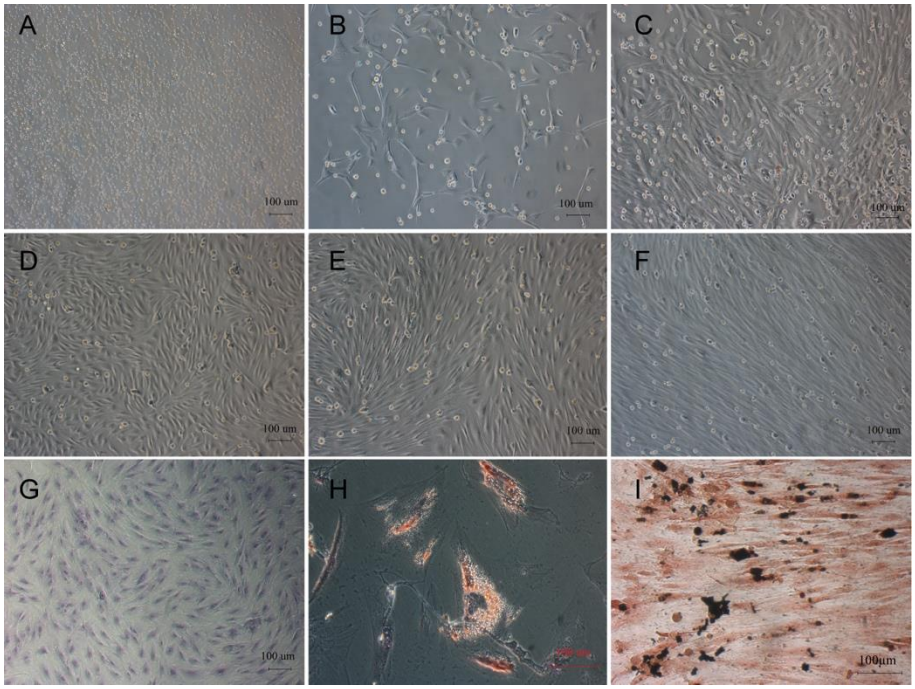

Figure 1. Isolation and identification of bone marrow mesenchymal stem cells (BMSCs). BMSCs at 1 day (**A**), 3 days (**B**), 5 days (**C**), 7 days (**D**), 9 days (**E**) incubation. BMSCs at passage 3 days (**F**). BMSCs by Giemsa staining (**G**). Lipogenic induction of BMSCs at 18 days by oil red O staining (**H**). Osteoblast induction of BMSCs at 21 days by Von- Kossa modified staining (**I**).

without inducers. Six parallel replicate wells were set up in each group, and the solution was changed twice a week. After 21 days of induction, the supernatant was taken and the bone forming protein 2 (BMP-2) content was measured according to the instructions of BMP-2 kit (Abnova, Walnut, CA, USA). The cells were fixed by 40 g/L paraformaldehyde. The induced mineralized nodules were subjected to Von-Kossa modified staining, and their numbers were observed microscopically [21, 22].

Statistical analysis

All data were shown as means ± SD and were analyzed by using SPSS 19.0 software (IBM, Ammon, NY, USA). Mean values were compared by using one-way analysis of variance (ANOVA) followed by Tukey's-b test to compare means among the different treatment groups. A significant difference was accepted as $P < 0.05$.

Results and discussion

Isolation and identification of BMSCs

By the inoculation of BMSCs in culture flasks, the cells were round in shape, varied in size, and suspended in the culture medium. After 24 h, some of the cells began to adhere to the wall, and were round, spindle-shaped, or polygonal (Figure 1A, 1B, 1C). The unadhered impurity cells were removed by fluid exchange. By 3-5 days of culture, radially arranged cell colonies with protrusions of varying length and thickness were visible with predominantly spindle-shaped cells, abundant cytoplasm, large nuclei, and clear nucleoli. From 6 to 7 days, the cells grew in colonies with 80% to 90% fusion in a swirling pattern and arranged in the same direction (Figure 1D). The cells were closely arranged and gradually fused into sheets from 9 to 10 days (Figure 1E). After digestion and passage, the passaged cells grew completely against the wall after 24 h. The cells were homogeneous in morphology with shuttle-shaped and vigorous cell growth. The cells then can be passaged once in four or five days. It can be stably passed continuously for more than 10 generations with

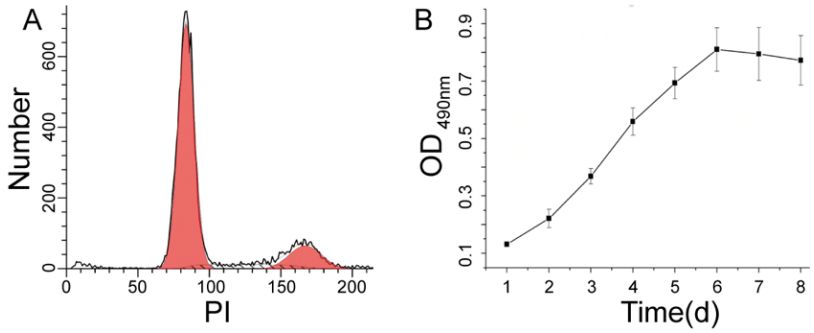

Figure 2. The cell cycle and growth curve of BMSCs. **A**: Cell cycle of BMSCs. **B**: Growth curve of BMSCs.

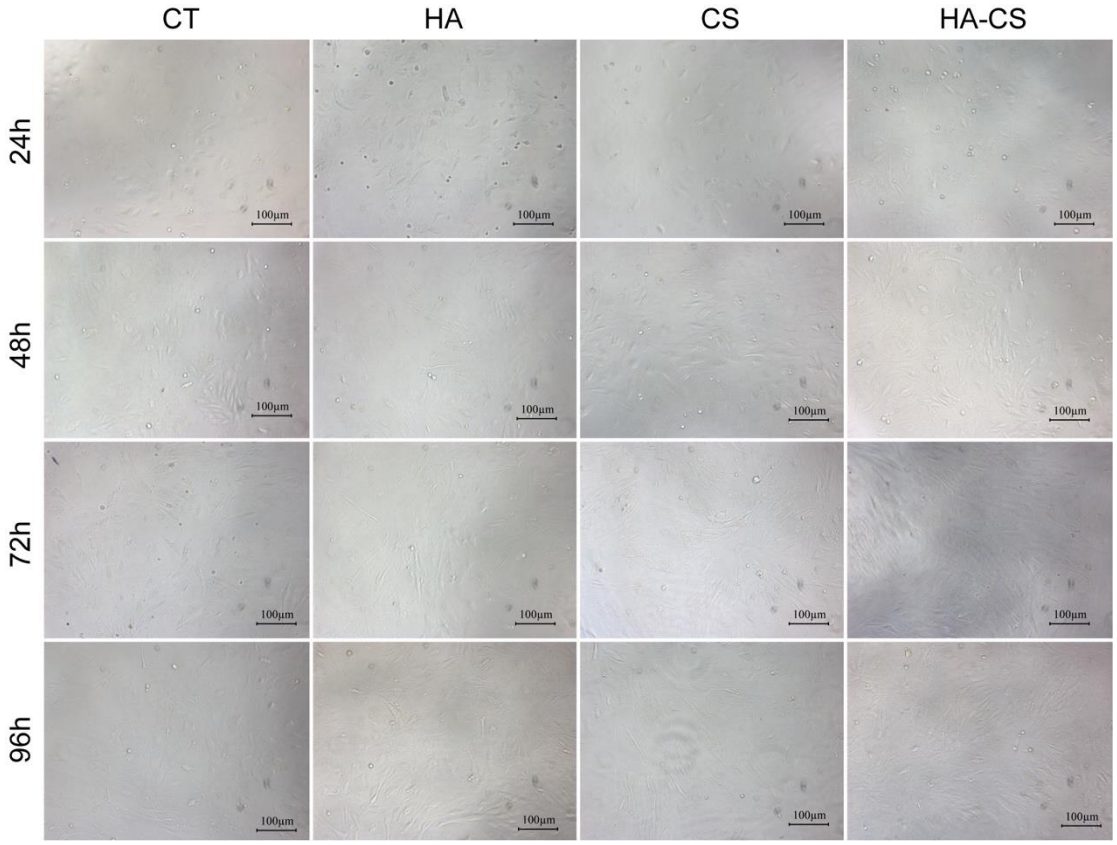

Figure 3. Effects of HA-CS on the cell morphology of BMSCs.

no significant changes in cell morphology and growth rate (Figure 1F). Giemsa staining showed that BMSCs were mostly shuttle-shaped with abundant cytoplasm stained purple-blue and nuclei stained dark blue with one or two nucleoli and obvious nucleoli (Figure 1G). Analysis of the morphological observations of the cells growing against the wall showed that they were consistent with the characteristics of BMSCs [15-17]. Figure 1H showed that, after 18 days of BMSCs culture with lipogenesis inducer, the adipocytes induced to accumulate lipids. The lipid droplets became larger and merged in the shape of string beads and showed bright red color by Oil Red O staining. It can be speculated that BMSCs can differentiate toward adipocytes with good potential for lipogenic differentiation under the induction of lipogenesis inducing

solution. Figure 1I showed that BMSCs formed a large number of calcified nodules with mineral salt deposits in the mesenchymal cells by Von-Kossa modified staining, which indicated that BMSCs could differentiate towards osteoblasts with good osteogenic differentiation potential under the induction of osteogenic fluid, which is in line with the characteristics of BMSCs with multi-directional differentiation potential [22].

Cell cycle analysis showed that 77.03% of BMSCs were in G0/G1 phase, 14.75% in G2/M phase, and 8.22% in S phase (Figure 2A), which indicated that BMSCs had a strong ability to divide and proliferate and was consistent with the biological characteristics of BMSCs. The growth curve of BMSCs (Figure 2B) demonstrated a typical "S"-shaped growth curve, which indicated that BMSCs were latently adapted on the first or second day of inoculation. The growth curve was basically linear from day 3 to day 6 indicating the logarithmic growth period of the cells. The curve became gradually flat after day 7 with cell proliferation slowing down significantly and entering a stable phase, which was consistent with the growth characteristics of BMSCs [15, 23]. The results confirmed that BMSCs were successfully isolated and purified by using whole bone marrow adherent method *in vitro*.

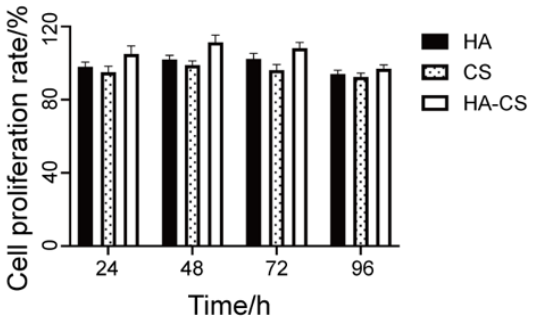

Figure 4. Effects of HA-CS on the proliferation of BMSCs.

Effect of HA-CS on the proliferation of BMSCs

With the extension of culture time, the cell number of BMSCs showed a significant increase and the cell morphology tended to gradually fuse into sheets (Figure 3). However, the differences in cell proliferation rates among all groups were not statistically significant (Figure 4), which indicated that HA, CS, and HA-CS were not toxic to BMSCs and had no significant effects on cell activity and proliferation, therefore, with a good biocompatibility.

Effect of HA-CS on the change of BMP-2 expression in BMSCs

Secretion and mineralization of extracellular matrix are essential parts of the bone formation process. BMP-2 is a highly efficient bone-producing factor [24]. The BMP-2 content in the culture medium after 21 d of induction was evaluated (Figure 5). All experimental groups were able to promote BMP-2 expression with the HA-CS group had the most significant effect.

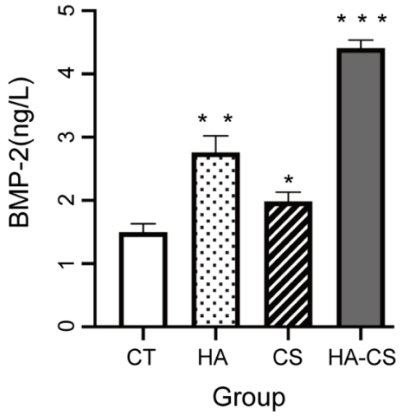

Figure 5. Effects of HA-CS on BMP-2 content. (Note: comparing to the control group (CT), *: $P < 0.05$; **: $P < 0.01$; ***: $P < 0.001$)

Effect of HA-CS on the number of calcified junction formation

At day 21 of induction, all experimental groups showed the formation of calcium nodules by Von-Kossa modified staining (Figure 6). Black mineralized particles were seen under the microscope in all groups with different sizes. Some areas of calcium nodules fused with each other to form sheets. In the control group (Figure 6A), the number of calcified nodules was low and sporadically distributed. However, in the HA and CS groups (Figure 6B and 6C), the black nodule-

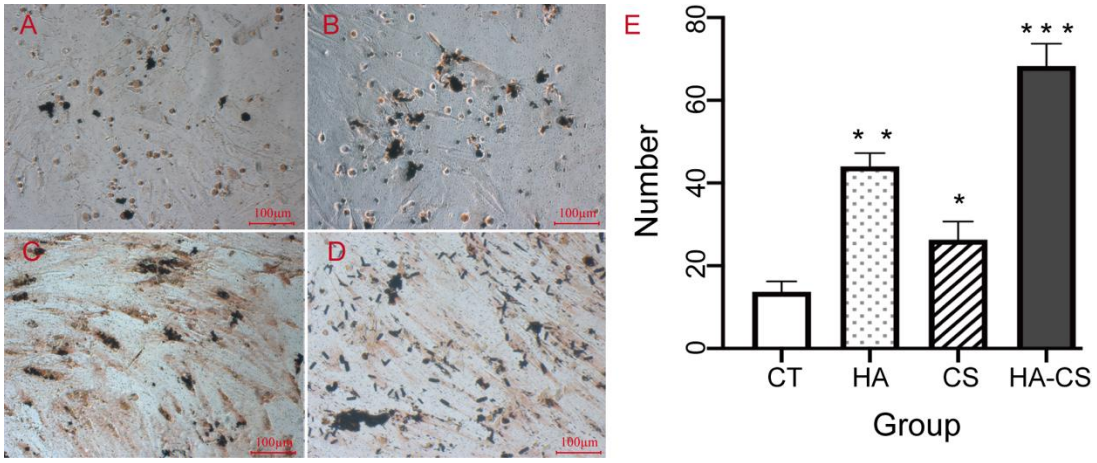

Figure 6. Effect of HA-CS on the number of calcified junction formation. **A**: blank control group. **B**: HA group. **C**: CS group. **D**: HA-CA group. **E**: calcified node count plot, comparing to the control group (CT). *: $P < 0.05$; **: $P < 0.01$; ***: $P < 0.001$.

like material was significantly larger. The mineralized particles were rounded, increased in number, and slightly fused. In the HA-CS group (Figure 6D), the mineralized particles were crystalline and densely distributed. Some areas were fused with each other to form sheets. The number and area of calcium nodules in each experimental group (HA, CS, and HA-CS) were significantly higher than that in the control group ($P < 0.05$). The differences between experimental groups were compared in Figure 6E with the most significant effect in the HA-CS group.

In contrast to isolation methods such as immunomagnetic bead method, flow cytometry isolation method, density gradient centrifugation method that require critical experimental conditions, high bone marrow demand, and isolation processes that affect cell activity, the whole bone marrow wall culture method used in this study is convenience, low cost, and maximum cell activity. The BMSCs can grow against the wall but hematopoietic stem cells cannot. Therefore, the suspended hematopoietic cells can be removed by changing the cell culture medium several times to obtain isolated, culturable, and purified BMSCs [15-17]. The results of morphological observation, cell cycle, growth curve, and multi-directional differentiation analysis of isolated cells by whole bone marrow apposition isolation method in this study demonstrated that rabbit primary cells adhered to the wall after being cultured for 24 h, and the adherent cells were basically covered the culture dish from 7 to 10 days. Matured cells showed abundant cytoplasm, stained purple-blue, dark blue stained nuclei, with one or two obvious nucleoli. The cells were mostly shuttle-shaped, swirl-like or fish-like distribution, and tended to grow in clusters. About 77.03% of cells were in G0/G1 phase, 14.75% in G2/M phase, and 8.22% in S phase with the potential to differentiate into adipocytes and osteoblasts, which indicated that those cells were consistent with the characteristics of BMSCs [16, 23].

Osteogenic protein is a multifunctional growth factor. 43 members of the osteogenic protein family have been identified, of which osteogenic protein 2 is the most potent osteoinductive factor that promotes osteogenesis by regulating the expression of alkaline phosphatase, type I collagen, osteocalcin, osteopontin, and other genes, and is a decisive cytokine in the osteogenesis process [10, 25]. In this study, HA, CS, and HA-CS all significantly promoted the expression of osteoblast marker protein (osteogenic protein 2). HA-CS had the most significant effect, probably promoting the differentiation of BMSCs to osteoblasts by regulating the expression of osteogenic protein 2. Von-Kossa staining further verified that HA-CS

promoted the mineralization ability of BMSCs, because the most important marker of the differentiation of BMSCs to osteoblasts was the formation of calcified nodules. The results of Von- Kossa staining experiments showed that the number and area of calcium nodules were significantly higher in the HA-CS group than that in the control group.

Conclusions

HA-CS composites have good histocompatibility and promote the differentiation of BMSCs to osteoblasts, providing experimental data for HA-CS as a donor material for bone grafting and repair. However, the mechanism of its regulation of osteogenic differentiation of BMSCs is still unclear and will be further investigated in subsequent experiments to provide more basis for the clinical application of HA-CS.

Acknowledgements

This study was funded by the 2021 Fujian Provincial Science and Technology Commissioner Project (202135060046), 2022 Fujian Provincial Science and Technology Commissioner Project and the 2021 Innovation and Entrepreneurship Training Program for College Students in Fujian Province (S202110402077X) in People's Republic of China.

References

1. Cao GD, Pei YQ, Liu J, Li P, Liu P, Li XS. 2021. Research Progress on Bone Defect Repair Materials. Chin J Orthop Trauma. 34(4):382-388.
2. Le TM, Vu NB, Huynh PD, Van Pham P. 2021. Treatment of Osteochondral Femoral Head Defect by Human Umbilical Cord Mesenchymal Stem Cell Sheet Transplantation: An Experimental Study in Rats. Adv Exp Med Biol. doi: 10.1007/5584_2021_671. Epub ahead of print. PMID: 34739722.
3. Matheus HR, Ervolino E, Gusman DJR, Alves BES, Fiorin LG, Pereira PA, *et al*. 2021. Association of Hyaluronic Acid with a Deproteinized Bovine Graft Improves Bone Repair and Increases Bone Formation in Critical-Size Bone Defects. J Periodontol. 9211:1646-1658.
4. Xing F, Chi Z, Yang RX, Xu DR, Cui JF, Huang YF, *et al*. 2021. Chitin-Hydroxyapatite-Collagen Composite Scaffolds for Bone Regeneration. Int J Biol Macromol. 184:170-180.
5. Hile DD, Sonis ST, Doherty SA, Tian X, Zhang Q, Jee WS, *et al*. 2005. Dimensional Stability of the Alveolar Ridge after Implantation of a Bioabsorbable Bone Graft Substitute: A Radiographic and Histomorphometric Study in Rats. J Oral Implantol. 312:68-76.
6. Li JY, Zhu B, Zhang YQ, Meng ZD. 2021. *In Vivo* Biological Safety Study of Porous Zinc Oxide/Hydroxyapatite Composite Materials. Chin J Rep Reconstr Surg. 35(7):847-854.
7. Wang WJ, Wang XQ, Wang YM, Tong CG. 2021. Clinical Study of Autologous Cartilage Transplantation Based on Nano-Hydroxyapatite in the Treatment of Talar Osteochondral Injury. J Nanosci Nanotechnol. 212:1250-1258.
8. Wongin S, Wangdee C, Nantavisai S, Banlunara W, Nakbunnum R, Waikakul S, *et al*. 2021. Evaluation of Osteochondral-Like Tissues Using Human Freeze-Dried Cancellous Bone and Chondrocyte Sheets to Treat Osteochondral Defects in Rabbits. Biomater Sci. 913:4701-4716.
9. Chen R, Chen HB, Xue PP, Yang WG, Luo LZ, Tong MQ, *et al*. 2021. Ha/Mgo Nanocrystal-Based Hybrid Hydrogel with High Mechanical Strength and Osteoinductive Potential for Bone Reconstruction in Diabetic Rats. J Mater Chem B. 94:1107-1122.
10. Zhu SB, Zhang XT, Chen X, Wang YO, Li SN, Qiu GX, *et al*. 2021. Nano-Hydroxyapatite Scaffold Based on Recombinant Human Bone Morphogenetic Protein 2 and Its Application in Bone Defect Repair. J Biomed Nanotechnol. 177:1330-1338.
11. Huang JL, Ma T, Tang H, Fan XY, Xu YQ. 2012. Vancomycin Cationic Liposome Combined with Nano-Hydroxyapatite/Chitosan/Konjac Glucomannan Scaffold for Treatment of Infected Bone Defects in Rabbits. Zhongguo Xiu Fu Chong Jian Wai Ke Za Zhi. 262:190-195.
12. Ren ML, Wang XQ, Hu M, Jiang Y, Xu DR, Xiang HB, *et al*. 2021. Enhanced Bone Formation in Rat Critical-Size Tibia Defect by a Novel Quercetin-Containing Alpha-Calcium Sulphate Hemihydrate/Nano-Hydroxyapatite Composite. Biomed Pharmacother. 146:112570.
13. Shen K, Liu XN, Qin HJ, Chai Y, Wang L, Yu B. 2021. Ha-G-Cs Implant and Moderate-Intensity Exercise Stimulate Subchondral Bone Remodeling and Promote Repair of Osteochondral Defects in Mice. Int J Med Sci. 1816:3808-3820.
14. Meng FG, Yang ZB, Long DB, Gu MH, Shang M, Zeng AY, *et al*. 2022. Hyaluronan Size Alters Chondrogenesis of Mesenchymal Stem Cells Cultured on Tricalcium Phosphate-Collagen-Hyaluronan Scaffolds. J Biomed Mater Res A. 110(4):838-850.
15. Li LS, Zhang H, Wang CJ, Cheng HB, An YH. 2010. Isolation Methods and Biological Characteristics of Bone Marrow Mesenchymal Stem Cells. J Clin Rehab Tiss Engin Res. 14(10):1869-1873.
16. Qiu R, Tang CK, Shao RX, Quan RF. 2017. Studies on the Extraction, Isolation, Culture and Biological Characteristics of Bone Marrow Mesenchymal Stem Cells (Bmscs) from Macaca

Mulatta. Zhejiang Chinese Medical University Xue Bao. 41(11):847-854.

17. Li XF, Zhao JM, Su W, Cui XR, Luo SX, Ma AG. 2011. Culture and Identification of Rat Bone Marrow Mesenchymal Stem Cells. J Clin Rehab TisS Engin Res. 15(10):1721-1725.
18. Song Q, Yan J, Guo XQ, Yao Q, Yu XB. 2010. Proliferation and Differentiation of Bone Marrow Mesenchymal Stem Cells Cultured on Hydroxyapatite/Collagen Composite Scaffolds. J Clin Rehab TisS Engin Res. 14(47):8795-8799.
19. Huang YJ, Zhang XM, Zhan JD, Yan ZJ, Chen DS, Xue XH, *et al*. 2021. Bone Marrow Mesenchymal Stem Cell-Derived Exosomal Mir-206 Promotes Osteoblast Proliferation and Differentiation in Osteoarthritis by Reducing Elf3. J Cell Mol Med. 2516:7734-7745.
20. Zheng YH, Xiong W, Su K, Kuang SJ, Zhang ZG. 2013. Multilineage Differentiation of Human Bone Marrow Mesenchymal Stem Cells *in Vitro* and *in Vivo*. Exp Ther Med. 56:1576-1580.
21. Ozdal-Kurt F, Tuglu I, Vatansever HS, Tong S, Sen BH, Deliloglu-Gurhan SI. 2016. The Effect of Different Implant Biomaterials on the Behavior of Canine Bone Marrow Stromal Cells During Their Differentiation into Osteoblasts. Biotech Histochem. 916:412-422.
22. Shen Y, Liu HX, Ying XZ, Yang SZ, Nie PF, Cheng SW, *et al*. 2013. Dose-Dependent Effects of Nicotine on Proliferation and Differentiation of Human Bone Marrow Stromal Cells and the Antagonistic Action of Vitamin C. J Cell Biochem. 1148:1720-1728.
23. Wang L, Shi SJ, Bai RP, Wang Y, Guo Z, Li DD. 2020. Biological Properties of Bone Marrow Stem Cells and Adipose-Derived Stem Cells Derived from T2dm Rats: A Comparative Study. Cell Biosci. 10:102.
24. Xu T, Wu X, Zhou Z, Ye Y, Yan CT, Zhuge NS, *et al*. 2020. Hyperoside Ameliorates Periodontitis in Rats by Promoting Osteogenic Differentiation of Bmscs Via Activation of the Nf-Kappab Pathway. FEBS Open Bio. 109:1843-1855.
25. Xu CF, Wang MJ, Zandieh-Doulabi B, Sun W, Wei LF, Liu YL. 2021. To B (Bone Morphogenic Protein-2) or Not to B (Bone Morphogenic Protein-2): Mesenchymal Stem Cells May Explain the Protein's Role in Osteosarcomagenesis. Front Cell Dev Biol. 9:740783.